

# Weakly coupled neutral gauge bosons at future linear colliders

A. FREITAS

*Fermi National Accelerator Laboratory, Batavia, IL 60510-500, USA*

## Abstract

A weakly coupled new neutral gauge boson forms a narrow resonance that is hard to discover directly in  $e^+e^-$  collisions. However, if the gauge boson mass is below the center-of-mass energy, it can be produced through processes where the effective energy is reduced due to initial-state radiation and beamstrahlung. It is shown that at a high-luminosity linear collider, such a gauge boson can be searched for with very high sensitivity, leading to a substantial improvement compared to existing limits from the Tevatron and also extending beyond the expected reach of the LHC in most models. If a new vector boson is discovered either at the Tevatron Run II, the LHC or the linear collider, its properties can be determined at the linear collider with high precision, thus helping to reveal origin of the new boson.

## 1 Introduction

Although the Standard Model, based on the gauge symmetry  $SU(3)\times SU(2)\times U(1)$ , is impressively successful in describing the existing high-energy experimental results, it is expected to be only the low-energy manifestation of a more fundamental theory, involving extended or additional gauge groups. The additional gauge interactions may arise for example in the framework of grand unified theories [1] or theories of dynamical symmetry breaking [2]. Even if the fundamental gauge symmetry is broken at a scale far beyond the electroweak breaking scale, the breaking to the Standard Model gauge group may occur in several steps and some subgroups may remain unbroken at a scale not far from the electroweak scale. Therefore it is interesting to study a possible additional neutral gauge boson  $Z'$  with mass below 1 TeV. Such a new gauge boson with a mass as low as the order of the  $Z$  mass is still in accordance with all experimental bounds if its couplings to the Standard Model fermions are very weak [3].

Current limits from searches at the Tevatron [4] exclude a "sequential  $Z'$  boson" (i.e. a  $Z'$  boson that has the same couplings as the Standard Model  $Z$  boson) with mass below 780 GeV. For smaller masses, the sensitivity towards smaller couplings increases. For  $Z'$  masses as low as 300 GeV or less, the Tevatron can exclude  $Z'$  bosons with production cross-sections that are about 100 times smaller than for a sequential  $Z'$  boson.

The LEP experiments could also place limits on neutral gauge bosons, but the LEP data has not been analyzed for weakly coupled  $Z'$  bosons. It is expected that the limits obtainable from LEP, normalized to a sequential  $Z'$  boson, will be slightly better but comparable to the Tevatron limits for  $Z'$  bosons with masses below 210 GeV [5].

The searches for a relatively light weakly coupled  $Z'$  boson could be improved by a future  $e^+e^-$  high-energy linear collider with high luminosity [6], if the  $Z'$  boson couples to electrons. This report estimates the reach of a linear collider for  $Z'$  masses of the order of 1 TeV, focusing on the case that the mass of the  $Z'$  boson is below the  $e^+e^-$  center-of-mass energy. The findings are compared to the reach of the LHC for neutral gauge bosons. In addition to the discovery potential of an  $e^+e^-$  collider, the capabilities of determining the couplings of the  $Z'$  boson are investigated. For the most part of the analysis, no assumptions are made about the specific model structure that gives rise to the  $Z'$  boson. However, as an example, one interesting class of models studied in Ref. [5], where the Standard Model is extended by only one additional  $U(1)$  gauge group and no extra fermions, is analyzed in more detail.

## 2 Direct $Z'$ production

In the general setup for this study it is assumed that mixing effects between the  $Z$  and  $Z'$  bosons, introduced through off-diagonal entries in the neutral gauge-boson mass matrix, are negligible. When both the  $Z$  and  $Z'$  bosons couple to the Standard Model fermions, there will also be kinetic mixing generated by loop contributions at higher orders. These mixing effects, however, can always be rotated away for on-shell momenta of the gauge bosons by diagonalizing the higher-order propagator matrix. For small  $Z$ - $Z'$  mixing, no important

bounds on the  $Z'$  boson arise from indirect constraints from  $Z$ -pole data.

In this case, the most stringent bounds are obtained from direct  $Z'$  production. If the coupling  $g_{Z'ff}$  of the  $Z'$  boson to fermions (or other possible decay products) is small, it will form a narrow resonance that is hard to discover in the process  $e^+e^- \rightarrow f\bar{f}$ . Very stringent constraints can be obtained for values of the  $Z'$  mass close to the center-of-mass energy,  $M_{Z'} \approx \sqrt{s}$ . When the width is smaller than the detector resolution and the beam energy spread, the production cross-section for  $M_{Z'} = \sqrt{s}$  can be expressed as

$$\int d(\sqrt{s}) \sigma[e^+e^- \rightarrow Z' \rightarrow f\bar{f}] = \frac{6\pi^2\Gamma_{Z'}}{M_{Z'}^2} \text{Br}(Z' \rightarrow e^+e^-) \text{Br}(Z' \rightarrow f\bar{f}), \quad (1)$$

where the integration is performed over one energy bin. For a narrow  $Z'$  resonance away from the nominal center-of-mass energy,  $|M_{Z'} - \sqrt{s}| \gg \Gamma_{Z'}$ , the sensitivity of the process  $e^+e^- \rightarrow f\bar{f}$  quickly decreases. As pointed out in [3, 5], the most stringent constraints for  $M_{Z'} < \sqrt{s}$  are obtained from the case where the invariant mass of the  $f\bar{f}$ -system is reduced by initial-state radiation, so that the  $Z'$  boson can still be produced on-shell,

$$e^+e^- \rightarrow Z' + n\gamma \rightarrow f\bar{f} + n\gamma. \quad (2)$$

The leading initial-state radiation effects due to large logarithms,  $L = \log s/m_e^2$ , can be included using the structure-function approach [7],

$$\sigma[e^+e^- \rightarrow f\bar{f} + n\gamma](s) = \int_0^1 dx_+ \int_0^1 dx_- G_{ee}(x_+, s) G_{ee}(x_-, s) \sigma[e^+e^- \rightarrow f\bar{f}](sx_+x_-), \quad (3)$$

with the structure functions up to order  $\mathcal{O}(\alpha^2 L^2)^*$  and including soft-photon exponentiation given by [8]

$$G_{ee}(x, Q^2) = \frac{\zeta_\alpha (1-x)^{\zeta_\alpha-1}}{\Gamma(1+\zeta_\alpha)} e^{-\gamma_E \zeta_\alpha + 3\alpha L/4\pi} - \frac{\alpha}{2\pi} L (1+x) - \frac{1}{2} \left( \frac{\alpha}{2\pi} \right)^2 L^2 \left[ \frac{1+3x^2}{1-x} \log x + 4(1+x) \log(1-x) + 5+x \right], \quad (4)$$

where  $\zeta_\alpha = \alpha(L-1)/\pi$  and  $\gamma_E \approx 0.577$  is the Euler constant. The additional photons usually escape in the direction of the beam pipe and will not be considered for the signal signature.

Besides initial-state radiation, beamstrahlung plays an important role for high-luminosity  $e^+e^-$  colliders. It also leads to an effective reduction of the invariant mass of the hard scattering process. In this work beamstrahlung effects have been included using the program *Circe* [10] for TESLA design parameters [11]. This program provides effective parameterizations of detailed multi-body simulations obtained from the code *Guinea-Pig* [12].

Both photonic initial-state radiation and beamstrahlung contribute to the effective cross-section for  $Z'$  production. The effect from beamstrahlung becomes particularly important

---

\*The leading-logarithmic QED structure functions are known to higher orders beyond  $\mathcal{O}(\alpha^2 L^2)$  [9], which is however not relevant for the level of precision of this study.

for  $Z'$  masses close to the center-of-mass energy, contributing up to about 50% of the cross-section. For smaller values of the ratio  $M_{Z'}/\sqrt{s}$ , the contribution from beamstrahlung reduces to a few percent compared to initial-state radiation. The relative importance of beamstrahlung also grows with increasing beam energy. For this study, the beamstrahlung effects have been investigated only for the TESLA accelerator proposal. Generally speaking, the NLC/JLC [13] and CLIC [14] linear collider designs generate slightly larger beamstrahlung effects than the TESLA design, especially towards the lower end of the beam energy spectrum, i.e. for small effective beam energies (see e.g. [10,15]). Therefore the search prospects for  $Z'$  bosons with  $M_{Z'} \ll \sqrt{s}$  are slightly better for the NLC/JLC and CLIC designs as opposed to the TESLA design. However, since in this region the cross-section is dominantly generated by initial-state radiation, the general results of this study remain valid also for these other accelerator designs.

The main background to the signal process (2) arises from fermion pair production through s-channel photon or  $Z$  boson exchange,

$$e^+e^- \rightarrow \gamma^*/Z^* + n\gamma \rightarrow f\bar{f} + n\gamma. \quad (5)$$

Additional backgrounds arise from processes with higher particle multiplicity in the final state, for example leptons in conjunction with additional neutrinos or four-quark final states from  $W$ -boson or tau pair production. For a realistic experimental analysis, the four-fermion backgrounds may play a non-negligible role and should be taken into account. Nevertheless, since these backgrounds are sub-dominant with respect to the process (5), they will not modify the discovery reach for a  $Z'$  boson in a significant way and are thus not included in the present study.

Both the signal (2) and background (5) contributions have been calculated using Monte-Carlo techniques including the initial-state radiation and beamstrahlung effects. No detector effects or experimental acceptances are taken into account in this study. The coverage of the  $Z'$  parameter space could be improved by running at different center-of-mass energies. Here the following scenarios are considered: (i) near the  $W$ -boson threshold with  $\sqrt{s} = 170$  GeV and integrated luminosity  $\mathcal{L} = 50 \text{ fb}^{-1}$  [16], (ii) near the  $t$ -quark threshold with  $\sqrt{s} = 350$  GeV and  $\mathcal{L} = 100 \text{ fb}^{-1}$  [17], (iii) a base-line high-energy design with  $\sqrt{s} = 500$  GeV and  $\mathcal{L} = 500 \text{ fb}^{-1}$  [6], and (iv) an upgraded high-energy version with  $\sqrt{s} = 1000$  GeV and  $\mathcal{L} = 1000 \text{ fb}^{-1}$ .

As a starting point, the cleanest decay channel,  $Z' \rightarrow \mu^+\mu^-$ , will be considered. The presence of a  $Z'$  boson would show up as a resonance peak in the  $\mu$ -pair invariant mass spectrum. For the detection of a narrow resonance, a good momentum resolution is therefore important. Here the parameters of the TESLA study [18] are taken, which envisages a momentum resolution of  $\Delta(1/p) = 5 \times 10^{-5} \text{ GeV}^{-1}$  in the central tracker region. For a muon pair, this number needs to be multiplied by two. Due to the boost from the initial-state photon, the muons are not always produced back-to-back. Therefore a conservative additional factor of two is included to accommodate for possible topological effects. Considering that the maximum energy of the muons is  $\sqrt{s}/2$ , one obtains for the resolution of the  $\mu$ -pair invariant mass:

$$\Delta E_{\mu^+\mu^-} = 5 \times 10^{-5} \text{ GeV}^{-1} \times s. \quad (6)$$

To compute the significance of a possible  $Z'$  signal, the invariant mass spectrum of the  $\mu$  pair is divided into bins of the size given by eq. (6). Due to the narrow width of weakly coupled  $Z'$  boson, the signal will appear as an excess in a single bin. The expected signal cross-sections as a function of the  $Z'$  mass are exemplified in Fig. 1 for a  $Z'$  boson with couplings that are 30 times smaller compared to the Standard Model  $Z$  boson,  $g_{Z'ff}/(g_{Zff})_{\text{SM}} = 30$ . In this case the signal cross-section is reduced by a factor 900 relative to a sequential  $Z'$  boson. Also shown is the background level from the processes eq. (5) in the given bin. With luminosities of a few hundred  $\text{fb}^{-1}$  one expects signal rates of 1000–10000 events for the depicted example, with background levels that are about one order of magnitude larger. The  $Z'$  boson is searched for by counting the events in each invariant mass bin and looking for an excess in one bin while vetoing significant deviations from the background expectation in the other bins. In order to determine the statistical significance that the excess in one bin is not a statistical fluctuation, a  $\chi^2$  test over all bins is performed.

For a viable event, the two muons are required to be in the main region of the detector,  $|\cos\theta_{\mu^\pm}| < 0.94$ , where  $\theta_{\mu^\pm}$  is the polar angle of the  $\mu^\pm$ . Taking into account these constraints, the projected reach of a linear collider for a  $Z'$  boson is shown in Fig. 2. The results are presented in terms of the product of production cross-section times branching ratio  $\text{Br}(Z' \rightarrow \mu^+\mu^-)$ , normalized to the case where the  $Z'$  couplings are identical to the Standard Model  $Z$  boson. As evident from the figure, by combining information from the various collider energies, a  $Z'$  boson with a signal rate that is about three orders of magnitude smaller than for a gauge boson with Standard Model  $Z$  couplings can be found throughout the range  $50 \text{ GeV} < M_{Z'} < 1 \text{ TeV}$ , except near the  $Z$  resonance.

The sensitivity can be increased by including other final-state channels. For the  $Z' \rightarrow e^+e^-$  channel, a similar sensitivity as for the  $\mu^+\mu^-$  channel is expected. While the  $e^+e^-$  channel is plagued by larger background contributions due to t-channel photon or  $Z$ -boson exchange, most of this background is peaked in the forward or backward regions of the detector. By restricting the signal to the central detector region, the background levels for the  $e^+e^-$  and  $\mu^+\mu^-$  channel roughly comparable. Under the assumption of lepton universality, the two lepton channels can be statistically combined, thus improving the limits in Fig. 2 by about a factor  $\sqrt{2}$ . The inclusion of the decay channel into taus,  $Z' \rightarrow \tau^+\tau^-$  is more demanding, because of the missing energy carried away by the neutrinos in the tau decays, and will not be considered here.

Depending on the branching ratios of the  $Z'$ , the inclusion of the decay channels into hadrons,  $Z' \rightarrow q\bar{q}$ ,  $q \neq t$ , can lead to stronger limits than the leptonic decay channels. Here only the decays into the five light quark flavors are considered, which are characterized by a two-jet signature. Due to the different decay signature of the top-quark, its contribution would have to be treated separately. However, a statistical combination with the light-quark channels is only possible using some assumptions about the underlying  $Z'$  model and will not be performed here. The resolution for the invariant mass spectrum of a jet pair is governed by the energy resolution of the hadronic calorimeter. The jet energy resolution for a jet with energy  $E$  is expected to be  $\Delta E/E = 35\%/\sqrt{E/\text{GeV}} \oplus 3\%$  [18], where  $\oplus$  indicates quadratic combination of the errors. By using again the maximal energy of the final-state jets,  $E_{\text{max}} = \sqrt{s}/2$ , one obtains the following (conservative) estimate for the resolution of

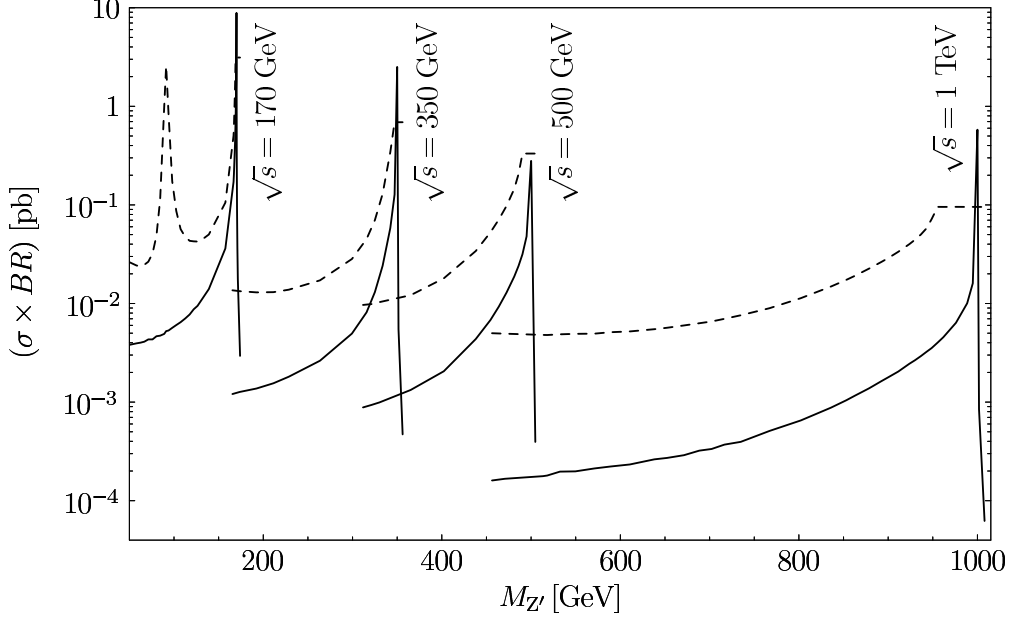


Figure 1: Signal cross-section times branching ratio (solid lines) in the  $\mu^+\mu^-$  channel for a sample  $Z'$  model with couplings that are 30 times smaller than for a sequential  $Z'$  boson. The cross-sections are shown as a function of the mass of the  $Z'$  boson,  $M_{Z'}$ , for different collider energies. Also shown is the background cross-section (dashed lines) in a bin in the  $\mu$ -pair invariant mass with a bin size given by eq. (6).

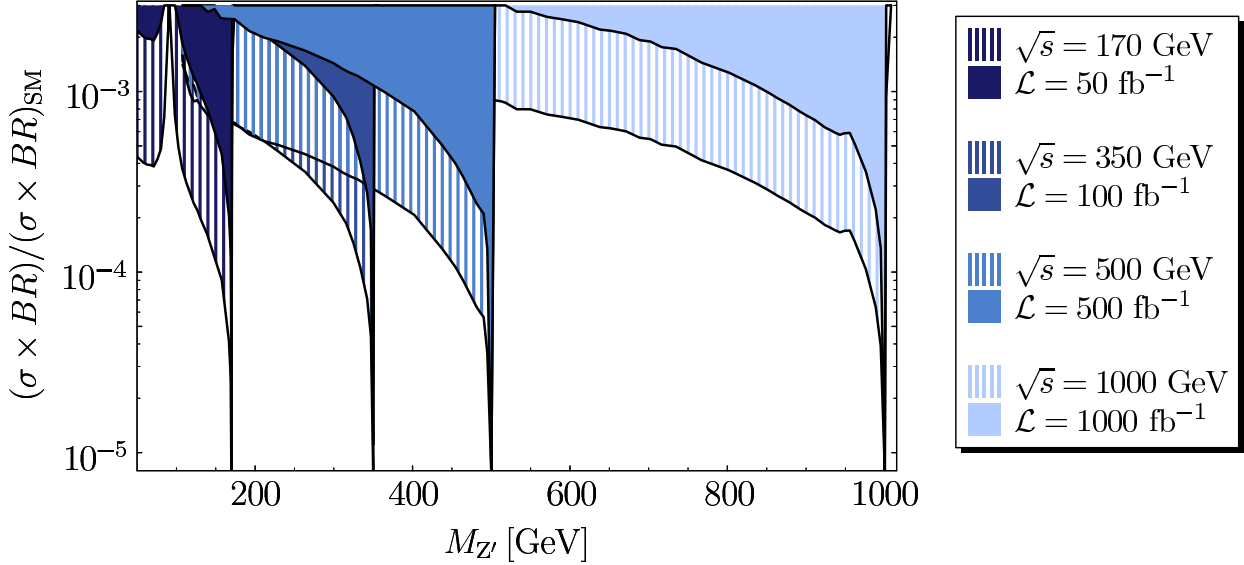


Figure 2: Projected sensitivity of a future  $e^+e^-$  collider for exclusion at 95% confidence level (hatched regions) and  $5\sigma$  discovery (solid regions) of an additional neutral gauge boson in the  $\mu^+\mu^-$  channel. Shown is the reach in terms of the product of production cross-section and branching ratio, normalized to the value for a Standard Model  $Z$  boson, as a function of the gauge boson mass,  $M_{Z'}$ , for various collider energies.

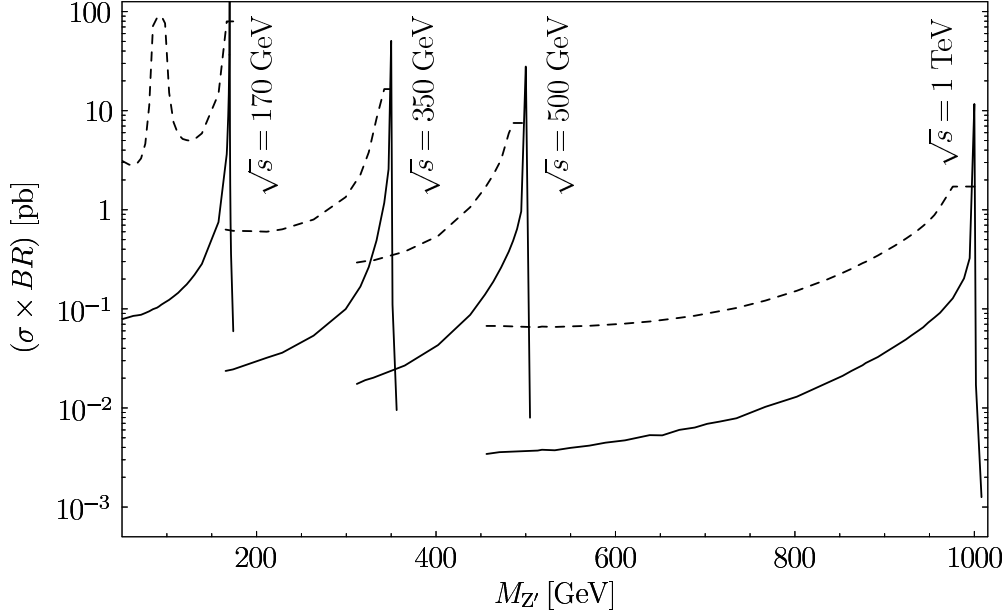


Figure 3: Signal cross-section times branching ratio (solid lines) in the di-jet channel for a sample  $Z'$  model with couplings that are 30 times smaller than for a sequential  $Z'$  boson. The cross-sections are shown as a function of the mass of the  $Z'$  boson,  $M_{Z'}$ , for different collider energies. Also shown is the background cross-section (dashed lines) in a bin in the di-jet invariant mass with a bin size given by eq. (7).

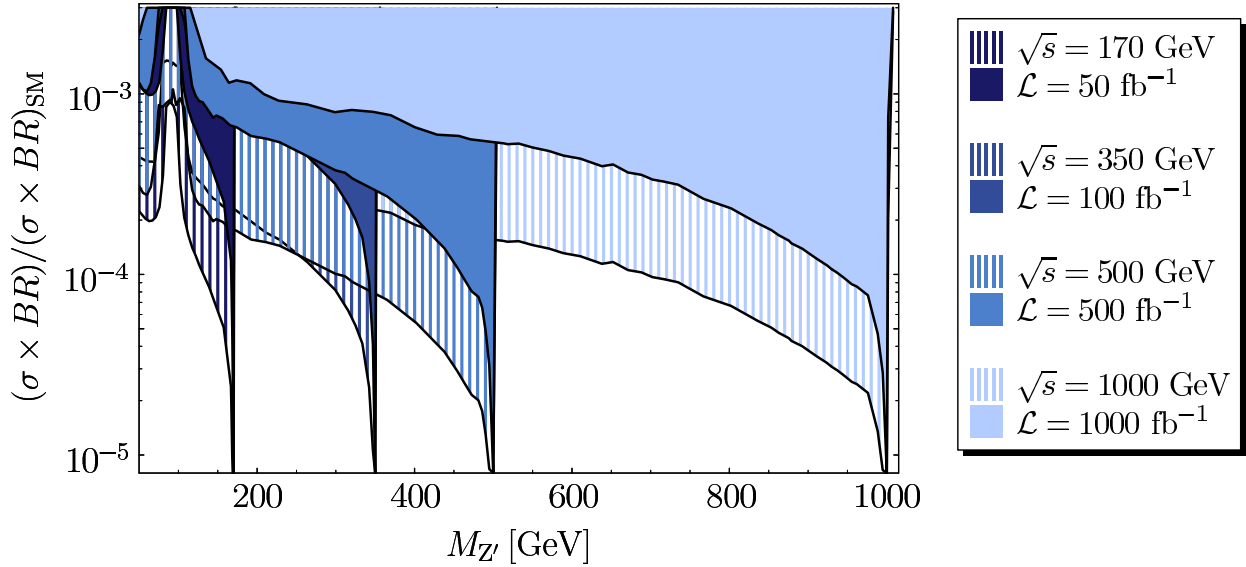


Figure 4: Projected sensitivity of a future  $e^+e^-$  collider for exclusion at 95% confidence level (hatched regions) and  $5\sigma$  discovery (solid regions) of an additional neutral gauge boson in the jet-jet channel. As in Fig. 2.

the di-jet invariant mass spectrum,

$$\Delta E_{jj} = 2 \sqrt{0.06125 \text{ GeV} \times \sqrt{s} + 0.000225 s}. \quad (7)$$

Similar to the muon channel, the signal is characterized by a narrow peak showing up as an excess in a single bin in a binned analysis of the di-jet invariant mass spectrum. As an example, Fig. 3 illustrates the expected signal and background cross-sections for a  $Z'$  boson with couplings that are 30 times smaller compared to the Standard Model  $Z$  boson and a bin size given by eq. (7).

Fig. 4 shows the expected sensitivity of a linear collider for a  $Z'$  boson in the hadronic decay channel. The improvement with respect to the  $\mu^+\mu^-$  channel is mainly a result of the normalization to the branching ratios of the Standard Model  $Z$  boson, which has relatively small couplings to the charged leptons,  $\text{Br}(Z \rightarrow \mu^+\mu^-) \approx 3.4\%$ , but large couplings to the quarks,  $\text{Br}(Z \rightarrow q\bar{q}) \approx 69\%$ .

It should be noted that besides the possibility to search for  $Z'$  boson in the decay channels into charged leptons and quarks, it is also possible to search for “invisible”  $Z'$  bosons, which primarily decay into neutrinos or other weakly interacting particles. The best limits for invisible  $Z'$  searches can be obtained from the process  $e^+e^- \rightarrow \gamma + \text{missing energy}$ , where a hard photon is required for tagging [19]. The presence of a  $Z'$  boson would show up as a resonance peak in the energy distribution of the photon. In contrast to the radiative-return method for visibly decaying  $Z'$  bosons, as discussed above, here the photon is not allowed to be in the kinematical region collinear to the beam pipe. As a consequence of this, the projected limits will be weakened by roughly a factor  $L = \log s/m_e^2$  compared to the discovery limits shown in Figs. 2, 4.

One of the most intriguing cases for the searches outlined above is the situation where only one  $Z'$  gauge boson but no evidence for other particles beyond the particle content of the Standard Model is found at future colliders. This situation has been studied in detail in Ref. [5]. The full gauge group of this model  $\text{SU}(3)_C \times \text{SU}(2)_L \times \text{U}(1)_Y \times \text{U}(1)_{Z'}$  extends the Standard Model gauge symmetry by an additional symmetry group  $\text{U}(1)_{Z'}$ , that is spontaneously broken by the vacuum expectation value of a new scalar field<sup>†</sup>,  $\phi$ . Under the assumption that mixing effects between the  $Z$  and  $Z'$  bosons are small, the  $Z'$  boson is directly associated with the  $\text{U}(1)_{Z'}$  group. The quantum numbers of the Standard Model quarks,  $q_L$ ,  $u_R$ ,  $d_R$ , and leptons,  $l_L$ ,  $e_R$ , and the Higgs doublet  $H$  are tightly constrained by anomaly cancellation (assuming generation-independent charges), leaving at most two independent parameters  $z_u$  and  $z_q$ , see Tab. 1. In general, these are further constrained depending on the number of right-handed neutrinos charged under  $\text{U}(1)_{Z'}$ . However, for the following discussion the right-handed neutrinos are assumed to be heavy and therefore irrelevant.

Neglecting the masses of the light fermions  $f$ ,  $f \neq t$ , the leading-order partial and total

---

<sup>†</sup>Note that the scalar  $\phi$  can easily escape observation when it is charged only under the additional gauge group  $\text{U}(1)_{Z'}$ , so that it couples to the Standard Model particles only through small mixing effects.

	SU(3) <sub>C</sub>	SU(2) <sub>L</sub>	U(1) <sub>Y</sub>	U(1) <sub>Z'</sub>
$q_L$	3	2	1/3	$z_q$
$u_R$	3	1	4/3	$z_u$
$d_R$	3	1	-2/3	$2z_q - z_u$
$l_L$	1	2	-1	$-3z_q$
$e_R$	1	1	-2	$-2z_q - z_u$
$H$	1	2	1	$-z_q + z_u$
$\phi$	1	1	0	1

Table 1: The most general allowed charge assignments for fermions and scalars under the extended gauge symmetry  $SU(3)_C \times SU(2)_L \times U(1)_Y \times U(1)_{Z'}$  when requiring anomaly cancellation and generation-blind couplings [5].

decay widths of the  $Z'$  boson read

$$\begin{aligned}
\Gamma[Z' \rightarrow \mu^+ \mu^-] &= \frac{g_{Z'}^2}{96\pi} M_{Z'} (13z_q^2 + 4z_q z_u + z_u^2), \\
\sum_{q \neq t} \Gamma[Z' \rightarrow q \bar{q}] &= \frac{g_{Z'}^2}{32\pi} M_{Z'} (17z_q^2 - 12z_q z_u + 5z_u^2), \\
\Gamma_{Z', \text{tot}} &= \frac{g_{Z'}^2}{32\pi} M_{Z'} (39z_q^2 - 8z_q z_u + 6z_u^2 + \delta\Gamma_t),
\end{aligned} \tag{8}$$

$$\delta\Gamma_t = \begin{cases} \sqrt{1 - 4\frac{m_t^2}{M_{Z'}^2}} \left[ (z_q + z_u)^2 \left( \frac{1}{2} + \frac{m_t^2}{M_{Z'}^2} \right) + (z_q - z_u)^2 \left( \frac{1}{2} - 2\frac{m_t^2}{M_{Z'}^2} \right) \right] & \text{for } M_{Z'} > 2m_t \\ 0 & \text{for } M_{Z'} < 2m_t, \end{cases}$$

where  $g_{Z'}$  is the gauge coupling associated with the gauge group  $U(1)_{Z'}$ . As evident from (8), the production and decay of the  $Z'$  boson is fully described by three unknown quantities, the mass  $M_{Z'}$  and the two products  $g_{Z'} z_u$  and  $g_{Z'} z_q$ . Taking the projected discovery limits in the  $\mu^+ \mu^-$  channel from Fig. 2, they can be translated into limits for the couplings  $g_{Z'} z_u$  and  $g_{Z'} z_q$ . Fig. 5 shows the discovery reach of a collider operating at  $\sqrt{s} = 1000$  GeV and  $\mathcal{L} = 1000 \text{ fb}^{-1}$  in terms of the couplings  $g_{Z'} z_u$  and  $g_{Z'} z_q$  for different  $Z'$  masses. Even for  $Z'$  masses that are substantially smaller than the center-of-mass energy, an impressive sensitivity for small  $Z'$  couplings can be achieved (for comparison, the Standard Model  $SU(2)_L$  coupling to left-handed quarks is  $|g_L^q| \approx 0.32$ ).

The discovery of a  $Z'$  boson could be translated into a band in the  $[g_{Z'} z_u, g_{Z'} z_q]$ -plane with the shape of the contours in Fig. 5. The two quantum numbers couplings  $g_{Z'} z_u$  and  $g_{Z'} z_q$  could be disentangled by examining in addition the branching ratios or the angular distribution of the decay products of the  $Z'$  boson.

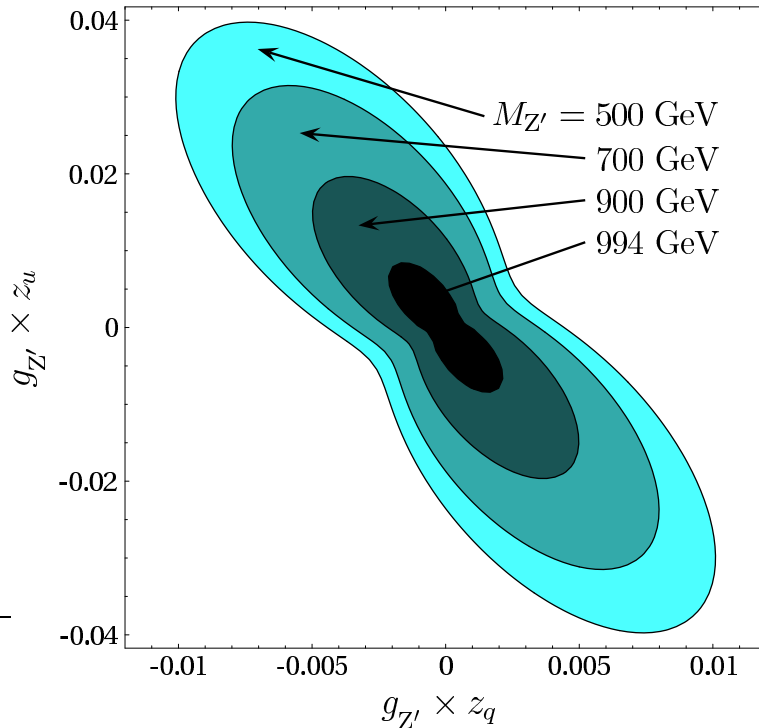


Figure 5: Discovery reach of a  $e^+e^-$  collider in the  $\mu^+\mu^-$  channel for  $\sqrt{s} = 1$  TeV in terms of the charges  $z_u$  and  $z_q$ , multiplied by the gauge coupling  $g_{Z'}$  of the extra U(1) group. The shaded areas indicate the remaining regions where a discovery is *not* possible for different values of the  $Z'$  mass.

### 3 Heavy $Z'$ bosons and comparison with hadron colliders

For  $Z'$  masses beyond the center-of-mass energy  $\sqrt{s}$ , the discovery sensitivity in the process  $e^+e^- \rightarrow f\bar{f}$  drops quickly. In this case, the presence of the  $Z'$  boson modifies the signal cross-section only through off-shell propagator effects. Nevertheless, for sufficiently strong  $Z'f\bar{f}$  couplings, a  $Z'$  boson can be discovered indirectly for masses much larger than  $\sqrt{s}$ . In Ref. [20] it has been shown for various grand unified models that the sensitivity of a linear collider extends to  $Z'$  masses which are about an order of magnitude larger than the center-of-mass energy.

For heavy gauge bosons, with  $M_{Z'} - \sqrt{s} \gg \Gamma_{Z'}$ , the contribution to the amplitudes for the process  $e^+e^- \rightarrow f\bar{f}$  essentially does not depend on the s-channel momentum transfer, i.e. the  $f\bar{f}$  invariant mass. Therefore the invariant mass spectrum of the final-state fermions is not a good observable for searching for heavy gauge bosons. Instead one can look for deviations in the integrated cross-section. Since in general the contribution of the  $Z'$  boson depends on the initial- and final-state helicities, it is useful to consider not only the total cross-section, but also the forward-backward, left-right and polarization asymmetries [20]. Nevertheless, for simplicity, in the following only the total cross-section for  $e^+e^- \rightarrow f\bar{f}$  will be considered.

These off-resonance searches for heavy  $Z'$  bosons can be combined with the direct searches

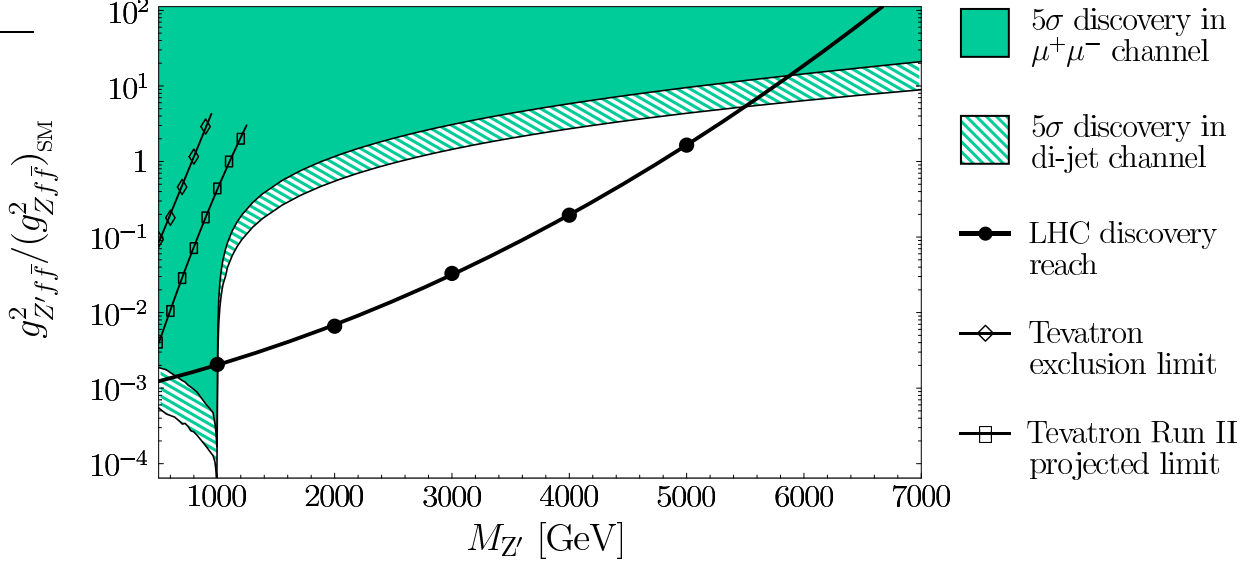


Figure 6: Projected discovery reach of a future  $e^+e^-$  collider with  $\sqrt{s} = 1000$  GeV and  $\mathcal{L} = 1000 \text{ fb}^{-1}$  for a sequential  $Z'$  boson in the  $\mu^+\mu^-$  and the di-jet channels. The depicted range of  $Z'$  masses includes direct and off-resonance searches (see text). Also shown are the discovery reach of the LHC [21] in the best channel  $Z' \rightarrow e^+e^-$ , the present limit from searches at the Tevatron [4] and the expected exclusion reach at the end of Tevatron Run II.

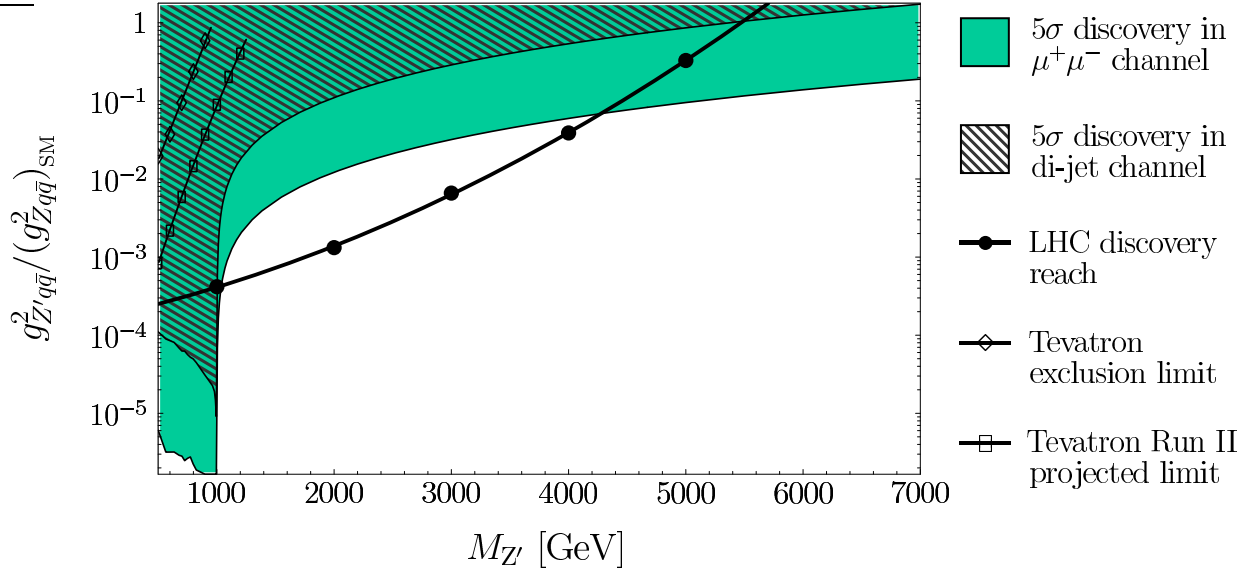


Figure 7: Projected discovery reach of a future  $e^+e^-$  collider with  $\sqrt{s} = 1000$  GeV and  $\mathcal{L} = 1000 \text{ fb}^{-1}$  for a  $Z_{B-L}$  boson in the  $\mu^+\mu^-$  and the di-jet channels. Also shown are the discovery reach of the LHC [21] in the best channel  $Z_{B-L} \rightarrow e^+e^-$ , the present limit from searches at the Tevatron [4] and the expected exclusion reach at the end of Tevatron Run II.

discussed above. Fig. 6 depicts the  $5\sigma$  discovery limits for a  $Z'$  boson with couplings that are proportional to the Standard Model  $Z$  boson ("sequential  $Z'$ ") in terms of the gauge coupling  $g_{Z'f\bar{f}}$  to the fermions, normalized to the Standard Model coupling. For  $M_{Z'} < \sqrt{s}$  the limits are derived from direct searches as in Figs. 2 and 4, while indirect searches using off-shell effects in the process  $e^+e^- \rightarrow f\bar{f}$  provide constraints for  $M_{Z'} > \sqrt{s}$ . Also shown are the coverage of the LHC [21] and the Tevatron [4] (for better visibility, the data points have been interpolated by smooth curves). The strongest constraints at hadron colliders are obtained from the decay  $Z' \rightarrow e^+e^-$ , since this channel offers the best momentum resolution [22]. The current limit from  $Z'$  searches at the Tevatron excludes  $Z'$  bosons with a production cross-section times branching ratio of more than  $\sim 40$  fb [4], leading to the exclusion contour in Fig. 6. This limit is expected to improve to  $\sim 2$  fb during the Run II of Tevatron, assuming an integrated luminosity of  $4 \text{ fb}^{-1}$ .

As can be seen from the figure, the linear collider provides very good sensitivity for  $Z'$  bosons with masses below  $\sqrt{s} = 1$  TeV and small couplings, and for very large values of  $M_{Z'}$ , but relatively strong couplings. In the intermediate region  $1 \text{ TeV} < M_{Z'} \lesssim 5.5 \text{ TeV}$ , the coverage of the LHC is superior, since here  $Z'$  bosons of this mass range can still be directly produced.

From a theoretical point-of-view, a more interesting case than the sequential  $Z'$  is a gauge boson with quantum numbers proportional to the difference between baryon number  $B$  and lepton number  $L$ . It is a special case of the minimal U(1) models summarized in Tab. 1 with  $z_q = z_u$ . The salient feature of such a  $Z_{B-L}$  boson is the fact that it does not mix with the Standard Model  $Z$  boson, so that constraints from  $Z$ -pole precision data on the  $Z_{B-L}$  boson are particularly weak. As pointed out before, in the absence of mixing in the tree-level mass matrix, mixing effects generated by higher-order loop contributions can always be rotated away for on-shell gauge bosons. The discovery reaches of a linear collider and the LHC for a  $Z_{B-L}$  boson are shown in Fig. 7, in terms of the  $Z'$  gauge coupling to the quarks,  $g_{Z'q\bar{q}}$ , normalized to the Standard Model  $Z$  coupling. Since a  $Z_{B-L}$  boson has a much larger branching ratio into leptons than a sequential  $Z'$ , the  $\mu^+\mu^-$  channel instead of the di-jet channel provides the best sensitivity for searches at an  $e^+e^-$  collider. In the high-mass region the linear collider can achieve better limits than the LHC already for  $Z'$  masses  $M_{Z'} \gtrsim 4.3$  TeV in this model.

## 4 Parameter determination

While the discovery potential for a  $Z'$  boson of a few TeV is superior at the LHC compared to a TeV linear collider, the linear collider can yield important information about the couplings of the  $Z'$  boson to the Standard Model fermions [20] and thus help to reveal the origin of the new gauge boson. Using the measurement of the  $Z'$  mass at the LHC as an input, the absolute values of the  $Z'$ -fermion couplings can be extracted through off-shell propagator effects even for  $M_{Z'} \gg \sqrt{s}$ . The reader is referred to Ref. [20] for more information.

In case of the discovery of a  $Z'$  boson with  $M_{Z'} < \sqrt{s}$  through the radiative-return method, the couplings of the new particle can be studied in detail by analyzing the branching ratios and angular and polarization asymmetries. The precision for these measurements can be

substantially enhanced by tuning the collider energy to the  $Z'$  resonance. Due to the high luminosity planned for a future linear collider, this would allow to measure the properties of the  $Z'$  boson with a level of precision comparable to the  $Z$ -pole measurements performed at LEP, even if the cross-section is several orders of magnitude smaller. In addition, the analyses can be improved by using polarized  $e^\pm$  beams.

A quantitative discussion of the parameter determination is only possible in the context of a specific model. In the following, the example of a  $Z_{B-L}$  boson with mass  $M_{Z'} = 400$  GeV and lepton coupling  $\tilde{g}_l = 0.006$  is considered. This model corresponds to a particular case of the minimal U(1) models listed in Tab. 1 with  $z_q = z_u$  and  $\tilde{g}_l = 3g_{Z'}z_q$ . As a special feature, the  $Z_{B-L}$  boson has only vector-like couplings to the Standard Model fermions, i.e. the couplings to left- and right-handed fermions are identical. The subsequent discussion will focus on the decay channel of the  $Z_{B-L}$  boson into muon pairs.

Using eq. (8) one obtains for the total width  $\Gamma_{Z'} \simeq 0.6$  MeV. The cross-section in the  $\mu^+\mu^-$  channel is computed from eq. (1) to be

$$(\sigma \times BR)/(\sigma \times BR)_{\text{SM}} \simeq 1.2 \times 10^{-3}. \quad (9)$$

As evident from Fig. 2, such a  $Z_{B-L}$  boson could be discovered at an  $e^+e^-$  collider running at  $\sqrt{s} = 500$  GeV and  $\mathcal{L} = 500 \text{ fb}^{-1}$  in the  $\mu^+\mu^-$  channel, while a  $5\sigma$  discovery at the LHC is not expected to be possible. Even in this case, in addition to the discovery of the new particle, it is also feasible to obtain valuable information about its parameters.

Due to the beam energy spread induced by beamstrahlung and initial-state radiation, the relatively small width of the new gauge boson,  $\Gamma_{Z'} \simeq 0.6$  MeV, cannot be directly resolved in a scan around the  $Z'$  resonance. As a consequence, absolute branching ratios and coupling parameters can only be determined by measuring all decay channels of the  $Z'$  boson, using photon tagging for the invisible decay modes as pointed out in section 2. While this method offers interesting perspectives for recognizing even exotic decay channels, the precision is limited due to the requirement of a transverse photon. It will be further explored at the end of this section.

Nevertheless, it is possible to determine ratios of couplings with high precision. For example, the ratio of the left-handed and right-handed coupling of the  $Z'$  boson to the electrons can be obtained by measuring the production cross-section for different polarizations of the incoming electron beam,

$$\left(\frac{g_{Z'ee}^L}{g_{Z'ee}^R}\right)^2 = \frac{(P+1)\sigma_L + (P-1)\sigma_R}{(P-1)\sigma_L + (P+1)\sigma_R}, \quad (10)$$

where  $\sigma_{L/R}$  is the cross-section for left-/right-polarized electrons and  $P$  is the polarization degree. In the special case of the  $Z_{B-L}$  boson the polarized cross-sections are identical,  $\sigma_L = \sigma_R$ , so that the determination of  $g_{Z'ee}^L/g_{Z'ee}^R$  is affected by the uncertainty in the polarization degree  $P$  only through statistical fluctuations. The resulting error is estimated to be of the order of  $10^{-4}$  and therefore negligible. The background contributions from Standard Model sources can either be computed using theoretical calculations or they can be obtained from measurements with a center-of-mass energy sufficiently far away from the

$Z'$  resonance, which are then extrapolated to  $\sqrt{s} = M_{Z'}$ . In both cases the systematic error of the background subtraction is relatively small and will not be considered henceforth.

In the given example, using  $10 \text{ fb}^{-1}$  each for left- and right-polarized  $e^-$  at  $\sqrt{s} = 400 \text{ GeV}$  and assuming a polarization degree of  $P = 80\%$  would result in  $N_{\text{sig}} \sim 22500$  signal events over a background of  $N_{\text{bkgd}} \sim 4700$  events for left-handed polarization and  $N_{\text{bkgd}} \sim 4000$  for right-handed polarization. The statistical error in the determination of the chiral electron couplings of the  $Z_{\text{B-L}}$  boson is then estimated to be

$$\frac{\delta(g_{Z'ee}^{\text{L}}/g_{Z'ee}^{\text{R}})}{g_{Z'ee}^{\text{L}}/g_{Z'ee}^{\text{R}}} \simeq 0.009. \quad (11)$$

The ratio of left- and right-handed couplings can also be extracted from the forward-backward asymmetry  $A_{\text{FB}}$ . It is defined as

$$A_{\text{FB}} = \frac{\sigma_{\text{F}} - \sigma_{\text{B}}}{\sigma_{\text{F}} + \sigma_{\text{B}}}, \quad \sigma_{\text{F}} = \int_0^{\cos \theta_{\text{max}}} d \cos \theta \frac{d\sigma}{d \cos \theta}, \quad \sigma_{\text{B}} = \int_{-\cos \theta_{\text{max}}}^0 d \cos \theta \frac{d\sigma}{d \cos \theta}, \quad (12)$$

where  $\theta$  is the scattering angle between the incoming  $e^-$  and the outgoing fermion  $f$ . Neglecting the mass of the final-state fermions, the forward-backward asymmetry for  $e^+e^- \rightarrow Z' \rightarrow f\bar{f}$  is expressed through the  $Z'$  couplings as follows,

$$A_{\text{FB}} = \frac{[(g_{Z'ee}^{\text{L}})^2 - (g_{Z'ee}^{\text{R}})^2][(g_{Z'ff}^{\text{L}})^2 - (g_{Z'ff}^{\text{R}})^2]}{[(g_{Z'ee}^{\text{L}})^2 + (g_{Z'ee}^{\text{R}})^2][(g_{Z'ff}^{\text{L}})^2 + (g_{Z'ff}^{\text{R}})^2]} \times \frac{\cos \theta_{\text{max}}}{1 + \frac{1}{3} \cos \theta_{\text{max}}}. \quad (13)$$

Considering the muon channel, i.e.  $f = \mu$ , and assuming lepton universality, the four couplings in eq. (13) are reduced to two independent couplings. Thus the ratio  $g_{Z'u}^{\text{L}}/g_{Z'u}^{\text{R}} = g_{Z'ee}^{\text{L}}/g_{Z'ee}^{\text{R}} = g_{Z'\mu\mu}^{\text{L}}/g_{Z'\mu\mu}^{\text{R}}$  can be determined from the forward-backward asymmetry in  $e^+e^- \rightarrow \mu^+\mu^-$  without using polarization up to a twofold ambiguity,

$$\left(\frac{g_{Z'u}^{\text{L}}}{g_{Z'u}^{\text{R}}}\right)^2 = \frac{\sqrt{C} - \sqrt{A_{\text{FB}}}}{\sqrt{C} + \sqrt{A_{\text{FB}}}} \quad \text{or} \quad \left(\frac{g_{Z'u}^{\text{L}}}{g_{Z'u}^{\text{R}}}\right)^2 = \frac{\sqrt{C} + \sqrt{A_{\text{FB}}}}{\sqrt{C} - \sqrt{A_{\text{FB}}}}, \quad \text{with} \quad C = \frac{\cos \theta_{\text{max}}}{1 + \frac{1}{3} \cos \theta_{\text{max}}}. \quad (14)$$

For the example of a  $Z_{\text{B-L}}$  boson, using  $20 \text{ fb}^{-1}$  and  $\cos \theta_{\text{max}} = 0.94$  would result in  $N_{\text{sig}} \sim 22500$  signal events each over a background of  $N_{\text{bkgd}} \sim 6500$  events for forward scattering and  $N_{\text{bkgd}} \sim 2200$  for backward scattering. This leads to the following statistical error for the determination of the  $Z_{\text{B-L}}$  couplings,

$$\frac{\delta(g_{Z'u}^{\text{L}}/g_{Z'u}^{\text{R}})}{g_{Z'u}^{\text{L}}/g_{Z'u}^{\text{R}}} \simeq 0.14. \quad (15)$$

This relatively poor precision is in part a result of the pathological case of the  $Z_{\text{B-L}}$  boson, which does not create any forward-backward asymmetry. The precision can be greatly improved by using the information about the  $Z_{\text{B-L}}$ -electron couplings from the polarized cross-section measurement (11) as an additional input. In this case it is also not necessary

to assume lepton universality. With this method a rather impressive statistical accuracy for the determination of the  $Z_{B-L}$ -muon couplings is achieved,

$$\frac{\delta(g_{Z'\mu\mu}^L/g_{Z'\mu\mu}^R)}{g_{Z'\mu\mu}^L/g_{Z'\mu\mu}^R} \simeq 0.01. \quad (16)$$

The propagation of the error in  $g_{Z'ee}^L/g_{Z'ee}^R$  from (11) leads to a negligible error in  $g_{Z'\mu\mu}^L/g_{Z'\mu\mu}^R$  of the order of  $10^{-4}$ , since for the  $Z_{B-L}$  coupling structure, this effect enters only through statistical fluctuations.

It is worth mentioning that, in addition to the asymmetry measurements, the ratio of the left- and right-handed couplings of the  $Z'$  boson to tau leptons can also be extracted from an analysis of the tau polarization, which can be extracted from the angular distribution of the hadronic decay products.

In a similar way, the ratios of the couplings to different fermion types, e.g. the ratio of the couplings to leptons and quarks,  $g_{Z'u}/g_{Z'qq}$ , can be determined at the per-cent level by comparing the cross-sections for lepton and jet pair production. If the  $Z'$  boson is not a  $Z_{B-L}$  boson, the coupling measurement (11) also depends on the uncertainty in the polarization degree. This uncertainty could be eliminated by using the Blondel scheme [23], if the positron beam can also be polarized.

Next the measurement of the mass of a narrow  $Z'$  boson will be discussed. Due to the limited energy resolution of the trackers and calorimeters, the most precise determination is achieved by measuring the cross-section at various center-of-mass energies around the  $Z'$  mass. While it is not possible to directly resolve the resonance line-shape of the  $Z'$  boson, as pointed out above, it is still possible to determine the mass of the boson accurately if the shape of the beam energy spectrum is precisely known. The effects of initial-state radiation have been calculated theoretically to high orders in perturbation theory [8, 9], so that the remaining theoretical uncertainty is negligible. The beamstrahlung effects due to interactions between the two incoming beams can be either obtained from numerical simulations based on theoretical models [12] or directly measured using Bhabha scattering [24].

Including beamstrahlung and initial-state radiation, Fig. 8 (a) shows the cross-section near the resonance peak for the  $Z_{B-L}$  model and three different values of the mass. As evident from the figure, the cross-section drops quickly for  $\sqrt{s} < M_{Z'}$ , but is smeared out for  $\sqrt{s} > M_{Z'}$  due to beamstrahlung and initial-state radiation. Thus by combining cross-section measurements below and above the nominal resonance peak, a strong sensitivity on the  $Z'$  mass is achieved.

As an example, the mass measurement of the  $Z_{B-L}$  boson with  $M_{Z'} = 400$  GeV from three measurements of the cross-section  $e^+e^- \rightarrow (Z_{B-L}) \rightarrow \mu^+\mu^-$  at  $\sqrt{s} = 399, 400, 401$  GeV is studied. The cross-section is computed including beamstrahlung and initial-state radiation and the cuts outlined in section 2. The dependence of the cross-sections on the mass at the three center-of-mass energies is depicted in Fig. 8 (b). Due to the beam energy spread, the cross-section at  $\sqrt{s} = 401$  GeV, i.e. above the mass peak, depends only mildly on the  $Z'$  mass. Nevertheless, it is useful to include this point as an absolute normalization for the other two other scan points, which depend more strongly on  $M_{Z'}$ .

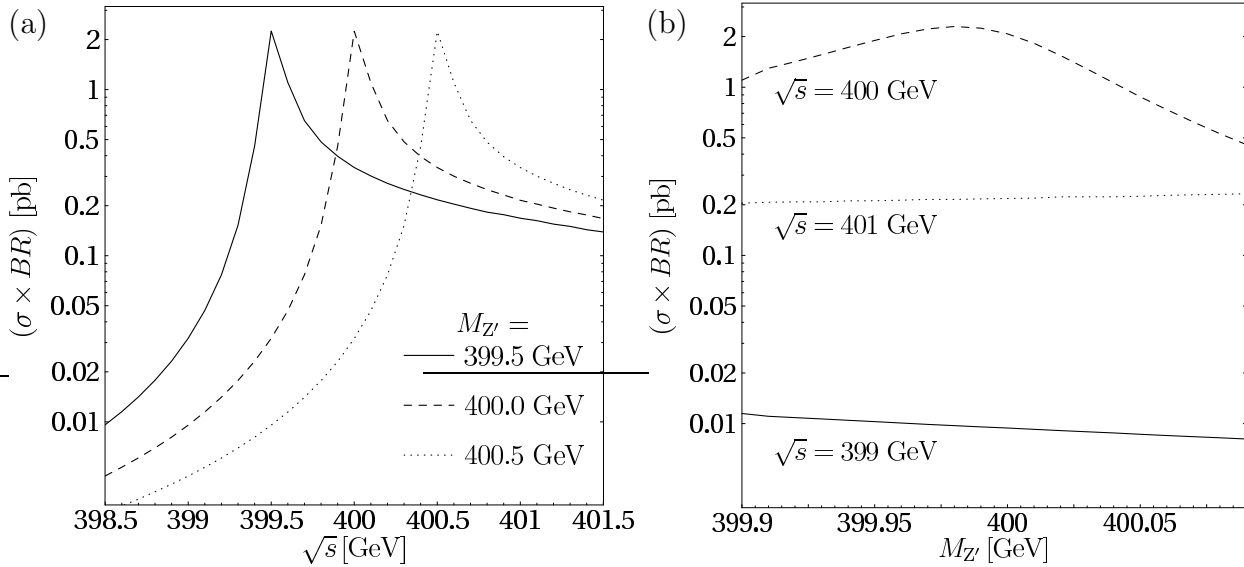


Figure 8: (a) Dependence of the cross-section for  $e^+e^- \rightarrow Z_{B-L} \rightarrow \mu^+\mu^-$  on the center-of-mass energy near the resonance peak for a  $Z_{B-L}$  boson with lepton coupling  $\tilde{g}_l = 0.006$  and different values of the mass. (b) Dependence of the cross-section for  $e^+e^- \rightarrow Z_{B-L} \rightarrow \mu^+\mu^-$  on the mass of the  $Z_{B-L}$  boson for three different center-of-mass energies.

It is assumed that  $10 \text{ fb}^{-1}$  is spent at each of the three center-of-mass energies. The mass is derived from the cross-section measurements by using a binned  $\chi^2$  fit with the mass and the lepton coupling,  $\tilde{g}_l$ , as unknown parameters (the unknown value of the total width can be absorbed into  $\tilde{g}_l$ ). In Fig. 9 the resulting one sigma contours are shown. The beam energy spread leads to a strong correlation between the mass and the coupling of the  $Z'$  boson. From the end-points of the contour in Fig. 9, the following estimate for the statistical errors of the mass determination is obtained,

$$M_{Z'} = 400.0^{+0.007}_{-0.013} \text{ GeV}. \quad (17)$$

At this high level of precision, the mass measurement error is dominated by systematic uncertainties. The absolute value of the beam energy is expected to be controllable at the level of  $10^{-4}$  or better [18], leading to an error of 40 MeV in the  $Z'$  mass. An additional uncertainty arises from the beamstrahlung spectrum. The beamstrahlung spectrum can be expressed through a simple parametrization introduced in Ref. [10],

$$G_{\text{beam}}(x) = a_0 \delta(1-x) + a_1 x^{a_2} (1-x)^{a_3}, \quad (18)$$

where  $x$  is the fraction of the beam energy in the collision process. From measurements of Bhabha events, the parameters  $a_i$  can be precisely determined, yielding for TESLA design parameters [24]

$$\begin{aligned} a_0 &= 0.5274 \pm 0.0014 \\ a_2 &= 13.895 \pm 0.082 \\ a_3 &= -0.6314 \pm 0.0021 \end{aligned} \quad \text{correlation matrix: } \begin{pmatrix} 1.000 & 0.430 & 0.708 \\ 0.430 & 1.000 & 0.755 \\ 0.708 & 0.755 & 1.000 \end{pmatrix}. \quad (19)$$

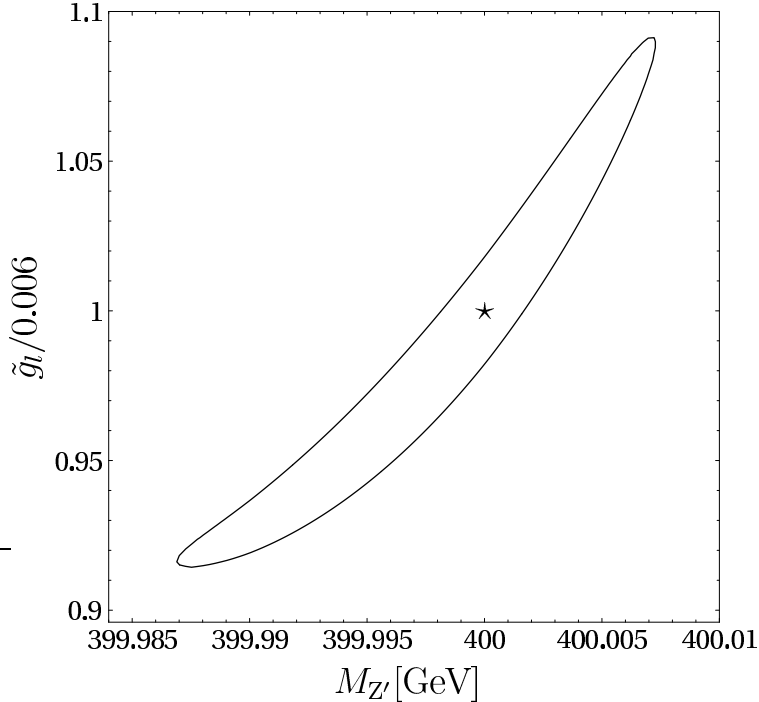


Figure 9: One sigma confidence level contours for the determination of the mass,  $M_{Z'}$ , and the leptonic coupling,  $\tilde{g}_l$ , of a  $Z_{B-L}$  boson with  $M_{Z'} = 400$  GeV and  $\tilde{g}_l = 0.006$ , obtained from simulated measurements of the cross-section  $e^+e^- \rightarrow (Z_{B-L}) \rightarrow \mu^+\mu^-$  at three center-of-mass energies,  $\sqrt{s} = M_{Z'}, M_{Z'} - 1$  GeV,  $M_{Z'} + 1$  GeV. The star indicates the values of the underlying model. The vertical axis for the leptonic coupling,  $\tilde{g}_l$ , is normalized to its nominal value of  $\tilde{g}_l = 0.006$ . In practice, due to the unknown value of the total  $Z_{B-L}$  width, this coupling could be determined only in arbitrary units.

The fourth parameter  $a_1$  is given by the normalization condition  $\int_0^1 dx G_{\text{beam}}(x) = 1$ . The influence of the uncertainty of the beamstrahlung spectrum on the mass determination has been estimated by folding the parametrization (18) with the  $Z'$  resonance function, which has been approximated by a  $\delta$ -function. Taking the errors and correlations in (19), a rather small effect on the extracted mass of 1 MeV is obtained. Other error sources like the uncertainty in the determination of the luminosity of the selection efficiency have been checked to be negligible. The total error is dominated by the error in the beam energy determination, resulting in

$$M_{Z'} = 400.0^{+0.041}_{-0.042} \text{ GeV}. \quad (20)$$

Thus one can conclude from this simplified study that a mass measurement with a precision at the level of  $10^{-4}$  seems feasible.

If the couplings of a hypothetical  $Z'$  boson are stronger, it might already be discovered at the Tevatron Run II or the LHC. Nevertheless, in this case measurements at the linear collider can supply important information about the couplings and mass of the extra gauge boson. Besides increasing the precision with respect to measurements at hadron colliders,

the linear collider also can investigate observables that are inaccessible at hadron colliders.

In particular, if the total decay width of the  $Z'$  boson is of the same order of magnitude as the average beam energy loss due to initial-state radiation and beamstrahlung (which is a few GeV for  $\sqrt{s} \sim 500$  GeV), it may be directly resolved in a scan around the  $Z'$  resonance. As a consequence, the measurement not only of *relative*, but of *absolute* branching ratios would be possible.

Alternatively, absolute branching ratios can also be determined by making use of photon tagging for the invisible decay channels, as pointed out above. The precision of this method is limited due to the requirement of a sufficiently hard transverse photon. As a consequence there is no enhancement due to the large collinear logarithms  $L = \log s/m_e^2$  as for the visible decay channels. In addition, because the tagging photon requires some minimum energy, the collider energy cannot be tuned directly to the  $Z'$  resonance. Therefore it is not possible to determine total branching ratios of very weakly coupled  $Z'$  bosons, such as the example of a  $Z_{B-L}$  with lepton coupling  $\tilde{g}_l = 0.006$ .

For moderate coupling strength, however, the measurement of the invisible decay channel is feasible. In the following a  $Z_{B-L}$  boson with the same mass as before,  $M_{Z'} = 400$  GeV, but larger lepton coupling  $\tilde{g}_l = 0.1$  will be considered. The signal is characterized by a photon plus missing energy,  $e^+e^- \rightarrow \gamma + \cancel{E}$ . The photon is required to have a minimum energy of  $E_\gamma^{\min} = 10$  GeV and to be emitted at an angle with respect to the beam axis larger than  $\theta_\gamma^{\min} = 20^\circ$ .

For a  $Z_{B-L}$  boson, the invisible decay modes originate from decays into neutrinos. The invariant mass  $M_{\nu\bar{\nu}}$  of the neutrino pair can be deduced from the photon energy  $E_\gamma$ ,  $M_{\nu\bar{\nu}}^2 = s(1 - E_\gamma/\sqrt{s})$ . Accordingly, the resolution of the invisible mass spectrum is governed by the photon energy resolution of the electromagnetic calorimeter, which is expected to be [18]

$$\Delta E_\gamma/E_\gamma = 10\%/\sqrt{E_\gamma/\text{GeV}} \oplus 1\%. \quad (21)$$

As before, the photon energy spectrum is divided into bins of the size given by eq. (21), with the signal concentrated in a single bin.

It turns out that the signal  $e^+e^- \rightarrow Z_{B-L}\gamma \rightarrow \nu\bar{\nu}\gamma$  is maximized for a collider energy of about  $\sqrt{s} \approx 420$  GeV, resulting in  $N_{\text{sig}} \sim 5700$  events for  $100 \text{ fb}^{-1}$  luminosity. The main background arises from the Standard Model contributions to  $e^+e^- \rightarrow \nu\bar{\nu}\gamma$ , which are mediated by s-channel  $Z$ -boson exchange or t-channel  $W$ -boson exchange. For the bin size eq. (21), about  $N_{\text{bkgd}} \sim 20000$  background events are expected. This leads to a statistical uncertainty in the determination of the “invisible”  $Z'$  cross-section of 2.8%.

The main systematic uncertainties for this measurement arise from the parametric uncertainty of the  $W$ -boson mass in the Standard Model background and the modeling of possible conversion of the photon into  $e^+e^-$  pairs in the detector, leading to a total systematic error of 0.4% [19]. In addition, there is a theoretical uncertainty arising from the subtraction of the background. It is assumed that the Standard Model background can be calculated with an accuracy of 0.2%, which induces an error of 1.1% on the signal cross-section. Adding statistical and systematic uncertainties, the total error for the measurement of the “invisible”  $Z'$  cross-section in this example is 3.1%.

Decay channel	Simulated measurement	Relative error
$l^+l^-$	$0.469 \pm 0.0035$	0.8%
$q\bar{q}, q \neq t$	$0.261 \pm 0.002$	0.8%
$t\bar{t}$	$0.035 \pm 0.0003$	0.8%
$\nu\bar{\nu}$	$0.235 \pm 0.0055$	2.5%

Table 2: Expected precision for the determination of absolute branching ratios for a  $Z_{B-L}$  boson with  $M_{Z'} = 400$  GeV and lepton coupling  $\tilde{g}_l = 0.1$ . The leptonic branching ratio has been derived under assumption of lepton universality.

Combining the measurement of the invisible cross-section with measurements of the visible decay modes of the  $Z'$  boson, i.e. the leptonic and hadronic cross-sections, allows to determine absolute branching ratios. In principle, one could also use the same photon tagging method for the visible decay channels as for the invisible decays, thereby minimizing the systematic uncertainties and theoretical assumptions. However, a more precise determination of the visible decay modes can be achieved by tuning the collider energy to the  $Z'$  resonance, as described before. In fact the error of resonance measurements is negligible compared to the error of the invisible cross-section determination from  $e^+e^- \rightarrow Z_{B-L}\gamma \rightarrow \nu\bar{\nu}\gamma$ . The combination of the visible cross-section measurements on the resonance and the invisible cross-section measurement via photon tagging requires the inclusion of beamstrahlung and photon radiation spectra. These spectra can be controlled with a precision far better than 1%, leading to a negligible uncertainty for the branching ratios.

The resulting errors for the absolute branching ratios are summarized in Tab. 2. For the decay modes into leptons and light quarks, flavor universality has been assumed. As evident from the table, although the neutrino branching ratio in the given example can only be determined with an error of a few percent, the precision for the other branching ratios is better than 1%.

## 5 Conclusions

In summary, the prospects of a future high-luminosity linear collider for searches for a new neutral  $Z'$  gauge boson have been reexamined, for the case that the  $Z'$  boson decays (primarily) into charged Standard Model fermions  $f$ . As a novel feature, the capability of a linear collider for direct detection of narrow  $Z'$  resonances through radiative return to the  $Z'$  pole has been investigated. These direct searches provide an unparalleled sensitivity for weakly coupled  $Z'$  bosons, allowing the discovery for  $Z'f\bar{f}$  that are up to two orders of magnitude weaker than the couplings of the Standard Model  $Z$  boson. In comparison with the LHC, a linear collider provides the best coverage for  $Z'$  searches for masses  $M_{Z'}$  below the  $e^+e^-$  center-of-mass energy  $\sqrt{s} \lesssim 1$  TeV, while the reach of the LHC is superior for higher masses in the range  $1 \text{ TeV} < M_{Z'} \lesssim 5 \text{ TeV}$ . For very large masses  $M_{Z'} \gg 1$  TeV, the linear collider can again achieve competitive limits through indirect effects of off-shell  $Z'$  bosons in the process  $e^+e^- \rightarrow f\bar{f}$ .

This study provides a simple estimate of the capabilities of a future linear collider for  $Z'$  searches, without including experimental acceptances, systematic uncertainties or other detector-related effects and taking into account only the dominant background sources. While these effects could modify the predictions for the event rates at the order of 10–30%, the general picture will nevertheless remain the same in a more refined analysis.

If a weakly coupled  $Z'$  boson with  $M_{Z'} \lesssim 1$  TeV is discovered either at hadron colliders or the linear collider, the  $Z'$ -fermion couplings could be measured precisely by tuning the collider energy to the  $Z'$  resonance. Even if these couplings are several orders of magnitude smaller than the couplings of the Standard Model  $Z$  boson, couplings ratios and branching ratios could be determined at the per-cent level. The mass of the  $Z'$  boson could be determined with a relative error of about  $10^{-4}$ .

Finally, an  $e^+e^-$  collider provides unique opportunities for searching for exotic  $Z'$  bosons, for example “hadrophobic”  $Z'$  bosons, which couple to the Standard Model leptons, but not to the quarks, or “invisible”  $Z'$  bosons, which primarily decay into undetectable particles, e. g. neutrinos. In the latter case, the searches are based on the process  $e^+e^- \rightarrow \gamma +$  missing energy, using a hard photon for tagging.

## Acknowledgments

This work greatly benefited from inspiring ideas and careful proofreading of the manuscript by M. Carena, B. Dobrescu and M. Schmitt. The author is grateful to M. Schmitt and M. K. Unel for help on the Tevatron limits and to S. Mrenna for useful discussions. This work is supported by the U.S. Department of Energy under Contract DE-AC02-76CH03000.

## References

- [1] For a review, see P. Langacker, *Phys. Rept.* **72**, 185 (1981).
- [2] For a recent review, see C. T. Hill and E. H. Simmons, *Phys. Rept.* **381**, 235 (2003).
- [3] A. Leike, *Phys. Rept.* **317**, 143 (1999).
- [4] DØ coll., V. M. Abazov *et al.*, DØnote 4375-Conf (2004);  
D. Waters, talk given at the *19th Annual Lake Louise Winter Institute*, Lake Louise, Alberta (2004);  
see also A. Dominguez (on behalf of the CDF coll.) and R. Kehoe (on behalf of the DØ coll.), talks given at the Fermilab Joint Experimental-Theoretical Physics Seminar, Aug 8, 2003.
- [5] T. Appelquist, B. A. Dobrescu and A. R. Hopper, *Phys. Rev. D* **68**, 035012 (2003).
- [6] TESLA Technical Design Report, Part III, eds. R. Heuer, D. J. Miller, F. Richard and P. M. Zerwas, DESY-2001-11C [hep-ph/0106315];  
T. Abe *et al.* [American Linear Collider Working Group Collaboration], in *Proc. of the APS/DPF/DPB Summer Study on the Future of Particle Physics (Snowmass 2001)*,

- eds. R. Davidson and C. Quigg, SLAC-R-570 [hep-ex/0106056];  
 K. Abe *et al.* [ACFA Linear Collider Working Group Collaboration], KEK-REPORT-2001-11 [hep-ph/0109166].
- [7] E. A. Kuraev and V. S. Fadin, Sov. J. Nucl. Phys. **41** (1985) 466 [Yad. Fiz. **41** (1985) 733];  
 G. Altarelli and G. Martinelli, in *Physics at LEP*, eds. J. Ellis and R. Peccei (CERN-86-02), Vol. 1, p. 47.
- [8] F. A. Berends *et al.*, in *Z Physics at LEP 1*, eds. G. Altarelli, R. Kleiss and C. Verzegnassi (CERN-89-08), p. 89.
- [9] M. Skrzypek and S. Jadach, Z. Phys. C **49**, 577 (1991);  
 M. Skrzypek, Acta Phys. Polon. B **23**, 135 (1992);  
 M. Cacciari, A. Deandrea, G. Montagna and O. Nicosini, Europhys. Lett. **17**, 123 (1992);  
 M. Przybycień, Acta Phys. Polon. B **24**, 1105 (1993);  
 G. Montagna, O. Nicosini and F. Piccinini, Phys. Lett. B **406**, 243 (1997).
- [10] T. Ohl, Comput. Phys. Commun. **101**, 269 (1997).
- [11] TESLA Technical Design Report, Part I, eds. F. Richard, J. R. Schneider, D. Trines and A. Wagner, DESY-2001-11A, [hep-ph/0106314].
- [12] D. Schulte, CERN-PS-99-014.
- [13] N. Phinney (*ed.*) *et al.* [NLC Collaboration], in *Proc. of the APS/DPF/DPB Summer Study on the Future of Particle Physics (Snowmass 2001)* eds. R. Davidson and C. Quigg, SLAC-R-571;  
 N. Akasaka *et al.* [JLC Design Study Group], KEK-REPORT-97-1.
- [14] G. Guignard (*ed.*), *A 3-TeV  $e^+e^-$  linear collider based on CLIC technology*, CERN-2000-008.
- [15] O. Napoly, CERN-SL-92-28-AP.
- [16] G. Wilson, in *2nd ECFA/DESY Linear Collider Study* (2001), p. 1498, LC-PHSM-2001-009 [<http://www-flc.desy.de/lcnotes/>].
- [17] D. Peralta, M. Martinez and R. Miquel, in *Proc. of the International Workshop on Linear Colliders (LCWS 99)*, Sitges, Spain (1999).
- [18] TESLA Technical Design Report, Part IV, eds. T. Behnke, S. Bertolucci, R.D. Heuer and R. Settles, DESY-2001-011D.
- [19] M. Carena, A. de Gouvêa, A. Freitas and M. Schmitt, Phys. Rev. D **68**, 113007 (2003).
- [20] S. Riemann, in *2nd ECFA/DESY Linear Collider Study* (2001), p. 1451, LC-TH-2001-007 [<http://www-flc.desy.de/lcnotes/>].

- [21] ATLAS Technical Design Report, CERN/LHCC-99-15, p. 940.
- [22] P. Camarri *et al.*, in *Proc. of the Large Hadron Collider Workshop*, eds. G. Jarlskog and D. Rein, Aachen, Germany (1990), Vol. II, p. 709.
- [23] A. Blondel, *Phys. Lett. B* **202**, 145 (1988) [Erratum-ibid. **208**, 531 (1988)].
- [24] K. Mönig in *2nd ECFA/DESY Linear Collider Study* (2001), p. 1353, LC-PHSM-2000-060 [<http://www-flc.desy.de/lcnotes/>].